PDF_CHEM: fast simulations of the chemical ISM using probability distributions

Bisbas, T.G.; Dishoeck, E.F. van; Hu, C.-Y.; Schruba, A.; Bouscasse, L.; Kramer, C.; Gueth, F.

EPJ Web of Conferences **265**, 00013 (2022) https://doi.org/10.1051/epjconf/202226500013
Multi-line Diagnostics of the Interstellar Medium

PDFCHEM: **Fast simulations of the chemical ISM using probability distributions**

Thomas G. Bisbas[1,2,*], *Ewine* van Dishoeck[3,4], *Chia-Yu* Hu[3], and *Andreas* Schruba[3]

[1]I. Physikalisches Institut, Universität zu Köln, Zülpicher Straße 77, 50923 Köln, Germany
[2]Department of Physics, Aristotle University of Thessaloniki, 54124 Thessaloniki, Greece
[3]Max-Planck-Institut für Extraterrestrische Physik, Giessenbachstrasse 1, 85748 Garching, Germany
[4]Leiden Observatory, Leiden University, P.O. Box 9513, 2300 RA Leiden, The Netherlands

Abstract. We present PDFCHEM, a new numerical method able to compute the photodissociation region (PDR) chemistry of large-scale inhomogeneous ISM regions using probability distributions of physical parameters as an input. We distinguish between two visual extinctions, namely the 'effective' ($A_{\rm V,eff}$) referring to the local extinction and the 'observed' ($A_{\rm V,obs}$) referring to the extinction taken from observations. Using 1,200 pre-calculated PDR simulations, we apply PDFCHEM to two hypothetical $A_{\rm V,obs}-$PDFs, representing a diffuse region and a Giant Molecular Cloud. PDFCHEM is fast and can replace the computationally expensive hydrodynamical models in understanding the chemistry of the ISM in different environments, including at low metallicities and high cosmic-ray ionization rates.

1 Introduction

To understand the evolution of the cosmic star-formation process, we need to know the corresponding molecular mass content of the interstellar medium (ISM) [15]. One of the key issues is to determine the distribution of species of large-scale inhomogeneous ISM objects, including galaxies. Classical studies using photodissociation region chemistry (PDR; [10, 16]), approach these systems with one-dimensional slabs of some uniform density. However, the ISM is very complex with varying densities and temperatures and, thus, far from a simple one-dimensional slab. To include the observed ISM complexity in simulations, the community has developed advanced astrophysical and cosmological codes which couple the magneto-hydrodynamical ISM evolution with PDR chemistry. Although this is a significant advancement, the downside is that it is computationally very expensive and takes a prohibitively long time to use such codes to study the ISM in a variety of environmental combinations (e.g. cosmic-ray ionization rates, FUV intensities, metallicities).

On the other hand, a complex ISM structure can often be represented by a characteristic column-density distribution, the so-called N-PDF or $A_{\rm V}-$PDF [1, 12, 14] if we refer to the visual extinction. This provides an opportunity to use these distributions to mimic the ISM complex structure and calculate their corresponding chemistry with much simpler PDR models. Towards this, a new approach has been presented recently by [5]. Here, we extend this approach by introducing two new important features: i) by reducing the grid of

*e-mail: bisbas@ph1.uni-koeln.de | thomasbisbas.com

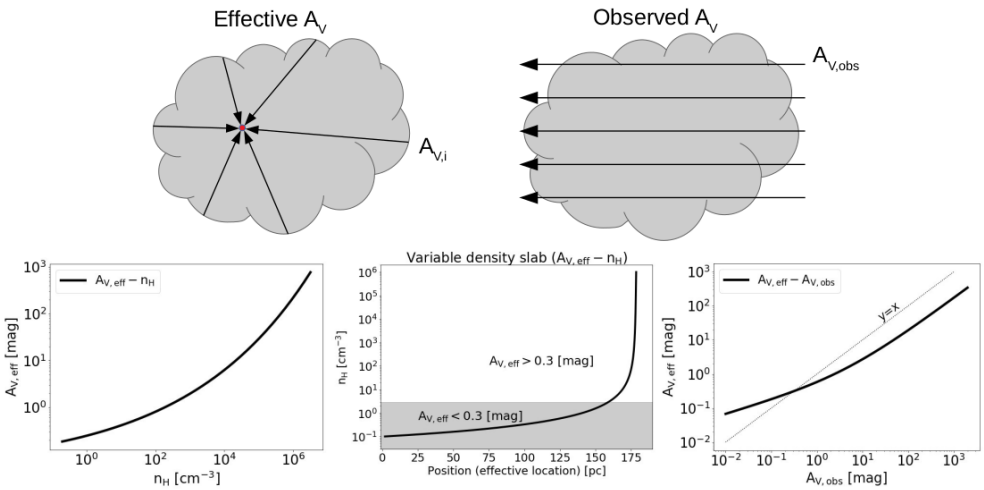

Figure 1. Top row: schematic showing the effective ($A_{\rm V,eff}$, left cloud) and the observed ($A_{\rm V,obs}$, right cloud) visual extinctions. Bottom row: the $A_{\rm V,eff} - n_{\rm H}$ (left panel), the variable density slab (middle panel) and $A_{\rm V,eff} - A_{\rm V,obs}$ relations (right panel). In the latter, the $y = x$ function is additionally plotted to guide the eye. This function is to represent the classical approach of $A_{\rm V,obs} \equiv A_{\rm V,eff}$.

one-dimensional uniform density slabs with *only one* variable density slab that represents a known connection between the local $A_{\rm V}$ and the local number density, and ii) by including radiative transfer calculations to compute the line emission of the most important coolants for any inputted $A_{\rm V}$−PDF under different combinations of ISM environmental parameters.

2 Numerical method and results

We distinguish between two visual extinctions: the 'effective' $A_{\rm V}$ (denoted as $A_{\rm V,eff}$), which represents the local visual extinction and it is the average of all $A_{\rm V}$ emanated from a computational cell of density $n_{\rm H}$ (see [9, 13]), and the 'observed' $A_{\rm V}$ (denoted as $A_{\rm V,obs}$), which represents the visual extinction along the line-of-sight of an observer. The top row of Fig. 1 shows a schematic of how $A_{\rm V,eff}$ and $A_{\rm V,obs}$ are defined. The bottom left panel shows the correlation of $A_{\rm V,eff} - n_{\rm H}$, which connects the local density with a most probable local visual extinction used for solving for the PDR chemistry (see [5, 11] for more details). From this relation, the variable density slab is constructed, which is shown in the bottom middle panel. The bottom right panel shows the $A_{\rm V,eff} - A_{\rm V,obs}$ relation. In the classical PDR approach, there is no distinction between $A_{\rm V,eff}$ and $A_{\rm V,obs}$. Instead they are assumed to be equivalent. This case is shown in dotted lines ($y = x$ function) in the latter panel and it deviates significantly from the presented $A_{\rm V,eff} - A_{\rm V,obs}$ relation [7]. It, therefore, alerts that *more special care must be taken when using observed column densities to perform PDR calculations*.

The publicly available code 3D-PDR[1] [2, 5], which treats the chemistry of PDRs in one- and three-dimensional clouds of arbitrary density distribution, has been used to construct a grid of 1,200 PDR simulations. For this grid, the variable density slab has been embedded in different combinations of ISM environmental parameters. In particular, we considered a cosmic-ray ionization rate in the range of $\zeta_{\rm CR} = 10^{-17} - 10^{-14}\,{\rm s}^{-1}$, an FUV intensity of $\chi/\chi_0 = 0.1 - 10^3$ normalized to the spectral shape of [8], and a metallicity of $Z = 1\,{\rm Z}_\odot$.

[1] https://uclchem.github.io/3dpdr/

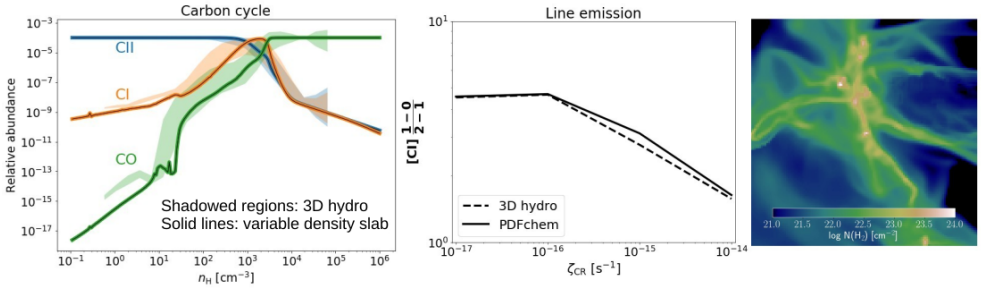

Figure 2. Comparison between the PDR calculations from the 3D hydrodynamical post-processed distribution. Left panel shows the carbon cycle (CII, CI and CO). The shadowed regions correspond to the 3D hydro calculations whereas solid lines show the corresponding results using the variable density slab. The middle panel shows the comparison between the 3D hydro (dashed) and PDFCHEM (solid) for the atomic carbon line ratio. The agreement is remarkable in all cases. The right panel shows the cloud used for the 3D hydro models (see [6] for further details on the 3D models).

PDFCHEM performs calculations in the following way: a) the user inputs the $A_{V,obs}-$PDF, b) each of the $A_{V,obs}$ is connected with a most probable n_H following the $A_{V,obs} - A_{V,eff}$ and $A_{V,eff} - n_H$ relations of Fig. 1, c) using the density distribution resulting from the $A_{V,eff} - n_H$ relation, each n_H is in turn connected to an effective position, r, up to which the column density of species and the radiative transfer calculations are evaluated for the requested combinations of ISM environmental parameters, d) steps (b)–(c) are repeated for every $A_{V,obs}$ followed by a weighted-average summation expressed in Eqn. (6) of [5].

Figure 2 benchmarks PDFCHEM against a 3D hydrodynamical post-processed simulation (see [6]), the density distribution of which is shown on the right panel. The left panel demonstrates the validity of using the variable density slab to replace the 3D-hydro PDR models. The middle panel shows the resultant ratio of atomic carbon lines for the 3D hydro model (dashed) and PDFCHEM (solid) as a function of ζ_{CR}. For the PDFCHEM, the $A_{V,obs}-$PDF relation of the 3D-hydro cloud was used (not shown). The agreement is remarkable in all cases.

Figure 3 shows preliminary results for two hypothetical distributions. The first is to represent a diffuse ISM region with $\overline{A_{V,obs}} = 1.0$ mag and a width of $\sigma = 0.5$ (top row). The second is a Giant Molecular Cloud with $\overline{A_{V,obs}} = 9.0$ mag and $\sigma = 0.8$ (bottom row; see Eqns.(2–5) of [5]). First and second columns show how the HI/2H$_2$ average abundance and the CO(1-0)/[CI](1-0) antenna temperature ratios, change for any $\zeta_{CR} - \chi/\chi_0$ combinations at $Z = 1\,Z_\odot$, respectively. The black solid line marks the HI/2H$_2$=1 ratio. The diffuse medium remains molecular only for $\chi/\chi_0 \lesssim 1$ and $\zeta_{CR} \lesssim 10^{-16}\,s^{-1}$. For these conditions, it is in general brighter in CO(1-0) than in [CI](1-0). On the other hand, the GMC remains molecular even for the highest values of ζ_{CR} and FUV intensities considered. It is brighter in CO(1-0) for $\zeta_{CR} \lesssim 10^{-16}\,s^{-1}$, however it becomes brighter in [CI](1-0) as ζ_{CR} increases. This effect of cosmic-ray induced destruction of CO has been studied by [3, 4, 6] and it makes the [CI](1-0) line an excellent alternative H_2 gas tracer particularly in systems permeated by high ζ_{CR}.

3 Conclusions

We present PDFCHEM, a new and fast method for determining the atomic and molecular mass contents of large-scale inhomogeneous clouds characterized by $A_{V,obs}-$PDFs. We distinguish between the effective (local) and the observed A_V and demonstrate that for more accurate PDR comparison with observations, a non-equivalent relationship between these two must be

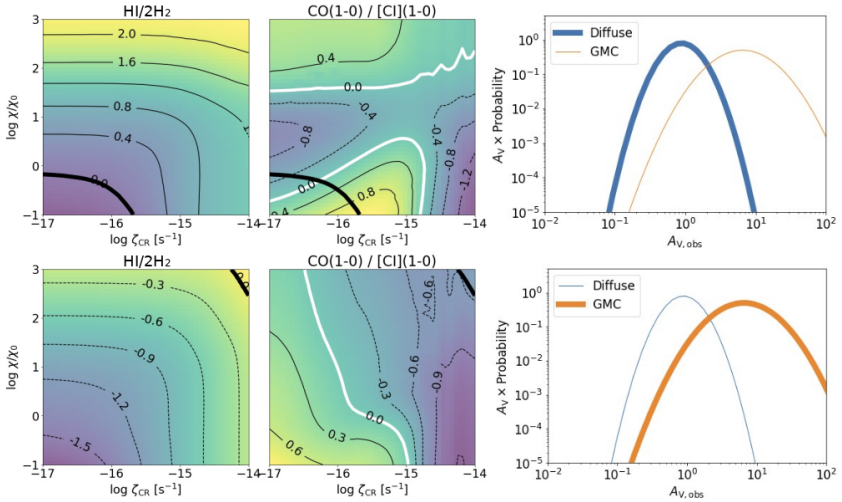

Figure 3. Top row corresponds to a hypothetical diffuse region and bottom row to a Giant Molecular Cloud. Their $A_{V,obs}$−PDFs are shown in the right column. The left column shows the PDF-averaged HI/$2H_2$ abundance ratio. The black solid line marks the condition HI/$2H_2$=1. Underneath of it, the distribution remains molecular. The middle column shows the antenna ratio of CO(1-0)/[CI](1-0). The white solid line shows the condition in which this ratio is equal to one. All contours are in log-space.

considered. Our simple 1D PDR models can reproduce the abundances and line emission results of complicated 3D hydro simulations, thus offering a much quicker alternative approach to study PDRs of complex systems. Our statistical method presented in [5] and expanded in this work can be used to estimate the PDR properties of large-scale ISM regions.

TGB acknowledges support from DFG grant No. 424563772. CYH acknowledges support from the DFG via German-Israel Project Cooperation grant STE1869/2-1 GE625/17-1.

References

[1] Abreu-Vicente J., Kainulainen J., Stutz A., et al. 2015, A&A, 581, A74
[2] Bisbas T. G., Bell T. A., Viti S., Yates J., Barlow M. J., 2012, MNRAS, 427, 2100
[3] Bisbas T. G., Papadopoulos P. P., Viti S., 2015, ApJ, 803, 37
[4] Bisbas T. G., van Dishoeck E. F., Papadopoulos P. P., et al., 2017, ApJ, 839, 90
[5] Bisbas T. G., Schruba A., van Dishoeck E. F., 2019, MNRAS, 485, 3097
[6] Bisbas T. G., Tan J. C., Tanaka K. E. I., 2021, MNRAS, 502, 2701
[7] Clark P. C., Glover S. C. O., 2014, MNRAS, 444, 2396
[8] Draine B. T., 1978, ApJS, 36, 595
[9] Glover S. C. O., Federrath C., Mac Low M.-M., Klessen R. S., 2010, MNRAS, 404, 2
[10] Hollenbach D. J., Tielens A. G. G. M., 1999, RvMP, 71, 173
[11] Hu C.-Y., Sternberg A., van Dishoeck E. F., 2021, ApJ, 920, 44
[12] Kainulainen J., Beuther H., Henning T., Plume R., 2009, A&A, 508, L35
[13] Offner S. S. R., Bisbas T. G., Viti S., Bell T. A., 2013, ApJ, 770, 49
[14] Schneider N., Bontemps S., Motte F., et al., 2016, A&A, 587, A74
[15] Tacconi L. J., Genzel R., Sternberg A., 2020, ARA&A, 58, 157
[16] Wolfire M. G., Vallini L., Chevance M., 2022, arXiv, arXiv:2202.05867